Abstract

Urban greening has been as a popular and effective strategy for ameliorating urban thermal 1 environment and air quality. Nevertheless, it remains an outstanding challenge for numerical 2 urban models to disentangle and quantify the complex interplay between heat and carbon 3 dynamics. In this study, we used a newly developed coupled urban canopy-carbon dynamics 4 model to investigate the environmental co-benefits for mitigating urban heat stress as well as the 5 reduction of carbon dioxide (CO₂) emission. In particular, we evaluated the impact of specific 6 7 components of urban greening, viz. fraction of the urban lawn, bare soil, tree coverage, and 8 irrigation, on heat and carbon fluxes in the built environment. The results of numerical simulations show that the expansion of urban green space, in general, leads to environmental 9 cooling and reduced CO₂ emission, albeit the efficacy varies for different vegetation types. In 10 11 addition, adequate irrigation is essential to effect plant physiological functions for cooling and 12 CO₂ uptake, while further improvement becomes marginal with excessive irrigation. The 13 findings of this study, along with its implications on environmental management, will help to 14 promote sustainable urban development strategies for achieving desirable environmental co-15 benefits for urban residents and practitioners.

16

- **Keyword:** Carbon emission; Environmental co-benefit; Mitigation strategies; Irrigation; Urban
- 18 greening; Urban vegetation

1 Introduction

19

20

21

22

23

24

25

26

27

28

29

30

31

32

33

34

35

36

37

38

39

40

41

Today, cities sustain more than half of the population in the world (UN 2019). The urbanization process converts natural land covers to engineered structures, leading to elevated ambient temperature, commonly known as the urban heat island (UHI) effect (Oke 1973; 1982). The urban thermal stress is further aggravated by anthropogenic heat emission (Sailor and Lu 2004; Sailor 2011), and synergistic interactions with synoptic-scale heat extremes (Perkins 2015; Wang et al., 2020). To foster urban environmental management, last decades have seen numerous heat mitigation strategies been proposed, including the use of innovative building and pavement materials, urban green (vegetation) or blue (water) infrastructure and design of urban morphology. The efficacy of heat mitigation strategies has been extensively evaluated using field observations as well as multi-physics multi-scale modeling from neighborhood to regional scales (Bowler et al., 2010; O'Malley et al., 2015; Yang et al., 2015a, 2016a, 2016b). It is noteworthy that most anthropogenic heat sources, such as vehicular emission and heating, ventilation, and air conditioning (HVAC) systems, are also significant contributors to greenhouse gases, especially carbon dioxide (CO₂). The elevated CO₂ concentration and deteriorated air quality in cities, in turn, tend to intensify the local UHI effect and further contribute to climate change at a global scale (Hutyra et al., 2014; Churkina 2016). In searching for the effective carbon mitigation strategies, much effort has been devoted to quantifying the anthropogenic releases of CO₂ via direct measurement, modeling, and inventory approaches (Crawford et al., 2011; Gately et al., 2015; Gately and Hutyra 2017; Sargent et al., 2018; Goret et al., 2019; Järvi et al., 2019). While it is well recognized that the anthropogenic CO₂ (AnCO₂) releases from fossil fuel consumptions dominate the overall carbon efflux in cities, many studies also pointed out that the biogenic CO₂ from urban greening spaces cannot be neglected (Vesala

et al., 2008; Bergeron and Strachan 2011; Hutyra et al., 2014). The carbon sequestration by urban vegetation (lawns, parks, golf courses, and residential gardens) can partially offset, e.g., the vehicular CO₂ emission. Some densely vegetated areas can achieve carbon neutral during warm months due to active plant CO₂ uptake (Bergeron and Strachan 2011).

Moreover, soils, as the growing media of vegetation and an indispensable part of urban green space, are often a net CO₂ source, (Koerner and Klopatek 2002; Tao et al., 2016). With urban warming and landscaping management, soil respiration rate is expected to be higher in cities than in the natural environment (Vesala et al., 2008; Decina et al., 2016; Dyukarev 2017; Contosta et al., 2020). Bare soil patches in degraded lawns due to inappropriate management release more CO₂ than bare soil land because of the continuing root and microbial respiration (Ng et al., 2015; Bae and Ryu 2017). Even with vegetation cover, Decina et al. (2016) found the annual soil respiration in a residential area with active landscaping management is comparable to the local traffic emissions in hot months, causing undesired effects on carbon reduction.

To achieve the desirable environmental co-benefit for mitigating both heat and carbon emissions by urban greening, holistic understanding of the physiological functions of urban vegetation is of pivotal importance. Theoretically, the rate of carbon release (respiration) and uptake (photosynthesis) from urban vegetation will be influenced by environmental temperature and soil water. The environmental cooling due to urban greening inhibits soil respiration and photosynthetic activities, working towards opposite directions in carbon budget. Similarly, urban irrigation provides additional water for plant growth and microbial respiration, which influences photosynthesis and respiration simultaneously. Whether urban greening (i.e. the expansion of vegetation fraction and irrigation) promotes or impedes CO₂ sequestration depends on the expansion rate and cooling efficiency, leading to possible trade-offs or co-benefits between

thermal and carbon mitigation. Based on in-situ observation or simple empirical models at neighborhood scale, previous studies revealed the importance of the complex interactions and feedbacks between urban green spaces and the built environment (Velasco and Roth 2010, Christen et al., 2011, Crawford et al., 2011, Velasco et al., 2013). Yet, the discussions were largely focused the singular impact on either thermal or carbon environment separately. Those focused on carbon exchange usually quantify the contribution of urban vegetation to the total CO₂ flux over the built terrain with fixed vegetation fraction and irrigation scheme, thus have limited abilities to examine the environmental response in terms of the alternation in land use and landscaping management strategies, as well as to guide future planning and decision making.

On the other hand, numerical models have the advantage over observational measurements by avoiding the limited timespans or footprints of measuring instruments, and number of sites, thus providing a versatile alternative approach to study the urban environment. Past decades have seen the development of numerous urban land surface models (LSMs) to simulate the dynamics and transport of heat and CO₂ emissions in the built environment (Arnfield 2003; Oke et al., 2017). In particular, numerical simulations at multi-scales, ranging from neighborhood to regional scales, were conducted to evaluate urban greening for cooling and energy saving, subjected to future trend of urbanization and global changes (e.g., Song and Wang 2016, Wang and Upreti 2019). From CO₂ exchange perspective, modeling technique has usually been applied to decompose the total CO₂ flux measured by eddy covariance system to identify the individual sector of the carbon source, but rarely discussed in the context of environmental co-benefit of heat mitigation. More recently, Li and Wang (2020, 2021) developed a novel urban modeling framework by integrating the urban carbon dynamics into a single-layer urban canopy model (hereafter referred to as the UCM-CO₂ model), where the biogenic CO₂ emission in urban

environment is captured using realistic plant physiological functions. This new UCM-CO₂ model hence enables us to quantify the synergistic environmental co-benefit of urban greening for both urban heat and CO₂ mitigation, arising from various sub-facets (i.e. pavements, lawns, shade trees, and bare soil).

The primary objective of this study is to examine the possible trade-offs or environmental co-benefits between heat and carbon mitigations provided by urban greening using the newly-developed UCM-CO₂ modeling framework. We simulate the changes in the ambient temperature, heat fluxes, and biogenic carbon exchange induced by varying four different components of urban greening, viz. the coverage of trees, grassland, bare soil, and the irrigation schedule. The relative contributions from each component are evaluated individually, while the collective result shows that urban greening could provide an overall environmental co-benefit of mitigation of both heat and carbon emissions. The results of this study will help to unravel the complex interactions among individual components of urban greening for ameliorating the total urban environmental quality.

2 Methods

2.1 The study area

In this study, we use the field measurements by an EC system located in west Phoenix, Arizona, USA (33.483847°N, 112.142609°W) to setup the base scenario as well as for the model calibration. The source area of the flux tower covers a typical residential area of single-family houses. The average roof height is 4.5 m, with a mean aspect (building-height-to-road-width, or H/W) ratio. Most lots in the study area have small front and backyard spaces with xeric

landscaping and irrigated with garden hoses or automated irrigation system. The overall land cover within 1 km² of the EC tower were 48.4% impervious surfaces (26.4% building and 22.0% road), 36.8% bare soil, 14.6% vegetation (10.1% grassland and 4.5% tree), and 0.1% water pool (Chow et al., 2014). The dominant vegetation species is Bermuda grass (a warm season C4 grass), while the common tree species are listed in Chow and Brazel (2012).

At the study site, the 23-m EC tower recorded four-components radiative fluxes, 3D wind field, air temperature, humidity, CO_2 flux and concentration, and pressure at 10 Hz frequency since 2011. The high frequency atmospheric measurements were then processed, quality-controlled, and integrated at 30 min intervals with no gap filling. To ensure sufficient mixing of CO_2 efflux, data points with the friction velocity u^* smaller than 0.1 m/s were removed from the observation. For numerical simulations, we used the measurements recorded from May 1 2012 to May 31 2012 (31 days).

2.2 The UCM-CO₂ model

The UCM-CO₂ model integrates the urban thermal and hydrological processes using a single-layer urban canopy model (UCM) (Wang et al., 2013; Yang et al., 2015b; Ryu et al., 2016, Wang et al., 2021) with the carbon exchange in the built environment (Li and Wang 2020, 2021). The geometry of the built environment is represented in the UCM as a two-dimensional (2D) street canyon, consisting of two arrays of buildings separated by a road, with infinite longitudinal dimension. Inside the street canyon, the heterogeneity of the ground facet is represented using sub-facets of paved surfaces (road), bare soil, and vegetated areas (lawns and trees). Furthermore, the morphological representation of urban trees in the UCM is made configurable to accommodate flexible location and number of rows of trees. The model resolves

explicitly the radiative heat exchange between shade trees and built facets (Wang 2014) and transpiration by tall vegetation, in addition to the ground level vegetation (lawns).

In addition, the new model is capable of resolving a holistic set of urban CO₂ uptake and emission arising from various sources, including human, building, and vehicular AnCO₂ emissions, plant biogenic CO₂ fluxes, and abiotic soil respiration, via a data fusion approach. The plant physiological functions parameterized in the UCM-CO₂ model resolves the dynamics of plants CO₂ exchange, including the carbon assimilation and respiration. Moreover, instead of using one set of plant parameters for all types of vegetations, UCM-CO₂ model distinguishes C₃ and C₄ plants to accommodate the simulation of urban lawns in arid/semi-arid area where warm season grassland is a norm in cities (Still et al., 2003; Trammell et al., 2019). The urban total energy and CO₂ fluxes are computed from the areal means of the sub-facets in the urban canyon.

For subsequent numerical simulations, we first configure the UCM-CO₂ model according to the landscape characteristics covering the source area of the EC flux measurements described in Section 2.1. The biogenic CO₂ exchange is captured by physiological functions of both C₃ and C₄ plants detailed in Li and Wang (2020). For example, the gross primary production at canopy level is calculated by integrating CO₂ uptake at leaf over the entire leaf surface area, as

$$A_{g,c} = \int_0^{LAI} A_g dL = A'_m \left(LAI - \frac{E_{int}}{K_x} \right), \tag{1}$$

where $A_{g,c}$ is the assimilation rate at canopy level; $A'_m = A_m + R_d$ with A_m the primary production and R_d the plant dark respiration; LAI is the leaf area index; K_x is the extinction coefficient; and E_{int} represents the overall leaf density from top to bottom of the canopy, calculated as

153
$$E_{\text{int}} = \text{Ei} \left[\frac{\alpha K_x \text{PAR}}{A'_m} \exp \left(-K_x \text{LAI} \right) \right] - \text{Ei} \left[\frac{\alpha K_x \text{PAR}}{A'_m} \right], \tag{2}$$

with Ei [•] the exponential integral, PAR the photosynthetic active radiation, and α the light use efficiency.

The CO₂ releases from anthropogenic sources are derived from the spatial gridded data. We use traffic on-road emission estimates from Vulcan v2.0 (10km, hourly, Gurney et al., 2009) and ODIAC (1 km, monthly, Oda et al., 2018), and further correct the daily traffic pattern using the local traffic count data in a nearby residential area from Arizona Department of Transportation (ADOT). Human respiration is calculated from population density while assuming normal level respiration rate per capita. Traffic release and human respiration from external data source are obtained from independent inventories and evaluated separately. The simulated hourly CO₂ along with the exchanges in each sector have been compared and calibrated against the EC measurement (Li and Wang 2020), and can be readily used by subsequent numerical experiments.

Based on the information of the morphology, land use, and EC measurement from the study site, the model is configured as shown in Table 1. It is noteworthy that the soil moisture was measured beneath the tower without irrigation, which did not accurately represent the soil moisture status in the source area of the EC measurements. In the neighboring residential area, the City of Phoenix recommends irrigating lawn at night or early morning every three days during summer and reduce to bi-weekly irrigation in winter (Landscape Watering by Numbers 2017). Since no information of actual soil moisture or irrigation in the study site is available, we derived the irrigation scheme from the municipal guidance of local residential irrigation and calibrated it against the measured latent heat from the EC tower. In this study, we use soil water content multiplier (SWC_x) to represent the overall irrigation scheme, which is defined as the ratio of target soil moisture after irrigation to the monthly mean soil moisture from measurement.

3 Results and discussion

3.1 Model validation

The UMC-CO₂ model was first calibrated and evaluated against the EC measurements from May 1st 2012 to May 31st 2012. The results of comparison of the net radiation (R_n), sensible heat (H), latent heat (LE), and total carbon flux (F_c) are shown in Fig. 1a and 1b. The model performance on R_n , H, and LE predictions is comparable to those reported in previous UCM studies (e.g. Grimmond et al., 2011; Meili et al., 2020). As for the performance of CO₂ modeling against EC measurement, there is a paucity of reported results in the literature. For example, Goret et al. (2019) combined UCM and on-site campaign data to model F_c at a city core and reported a root-mean square error (RMSE) of 0.67 mg m⁻²s⁻¹ between model simulations and field measurements. The Surface Urban Energy and Water Balance Scheme (SUEWS) proposed in Järvi et al. (2019) has the RMSE between 0.02 and 0.25 mg m⁻²s⁻¹ when evaluating the diurnal pattern of F_c in different seasons. In comparison, the RMSE of CO₂ flux predicted by the UCM-CO₂ model is 0.04 mg m⁻²s⁻¹ for the mean diurnal cycle (Fig. 1b).

The total CO₂ flux at the study site measures the composition of CO₂ release from fossil fuel burning, human respiration, soil respiration, and NEE from urban tree and lawns. At the study site, traffic release is the major contributor to CO₂ efflux, followed by soil respiration due to the large bare soil fraction (Fig. 1c). Soil respiration rate is validated using the observation data reported in Koerner and Klopatek (2002) at Phoenix residential area. Human respiration typically contributes 10% of total CO₂ efflux with limited uncertainty caused by population change of the study area (Fig. 1c). Direct validation of plant NEE is technically difficult due to the lack of useable observational data at the study site. With the validation of total CO₂ flux and other major sources, plant NEE is validated indirectly by the residual of the CO₂ budget. The

current study is focused on the biogenic CO₂ exchange, i.e., the variation of CO₂ exchange caused by urban greening.

3.2 Results of case study

For the subsequent case study to explore the impact of urban greening on urban cooling and biogenic CO₂ exchange, we keep the parameter space of the UCM-CO₂ model described in Section 3.1 (Table 1) intact, except four parameters viz. the ground vegetation fraction (f_V), tree crown coverage (f_T), bare soil fraction (f_S), and irrigation schedule (SWC_x). The variation of these four parameters corresponds to the changes in four components of urban greening, viz. (1) lawns, (2) urban trees, (3) bare soil, and (4) soil moisture statues reflective of urban irrigation.

The change of tree coverage is achieved by adjusting the tree crown size, ramping from 5 to 25% of the road width. The irrigation is scheduled at midnight, with *SWC*_x changing from 0.9 to 3.5, which is equivalent to 3% and 87% in normalized saturation degree, respectively. Since the ET arising from bare soil and grassland in the semi-arid environment is highly nonlinear with respect to the soil moisture state (Li and Wang 2019), the irrigation schedule supports the plant to meet 28% to 100% of the evaporation demand in the field. Figure 2 shows the relations between *SWC*_x, normalized saturation degree, and evaporation reduction factor.

3.2.1 Average heat and carbon mitigation by urban greening

We first assess the impact of urban greening on the mean air temperature and mean net biogenic ecosystem exchange (NEE) in the street canyon, viz. T_{can} and NEE_{can}, averaged over the entire simulation period; the results are shown in Fig. 3. By changing the fraction of urban green

space, the increase of tree coverage leads to much more effective cooling of canyon air temperature than the increase of lawn coverage (colormap in Fig. 3a). This is consistent to the result reported in an earlier study and can be attributed to the radiative shading by the 3D urban trees being more effective than evapotranspirative cooling by the 2D (planar) lawn (Wang et al., 2016). Ziter et al. (2019) also found the substantial temperature decrease when tree coverage is greater than 40%. As for the net carbon exchange inside the street canyon, we found that the urban green space, both trees and lawns, function as a net CO₂ sink even with the minimum coverage of f_V and f_T (5%) (contour in Fig. 3a). In general, the magnitude of NEE_{can} (with negative sign denoting carbon sink) further decreases with the urban tree and lawn fractions roughly linearly, signaling that the strength of urban green space as carbon sink increases. It is noteworthy that when f_T is large (> 0.15), the rate of NEE_{can} change with lawn fraction decays, indicating that lawns become weaker carbon sink in the presence of dense tree coverage. This can be physically interpreted as that tall/dense urban trees cast larger shaded areas on the ground and suppress the CO₂ uptake strength of the ground vegetation, by intercepting radiation (especially PAR) and lowering the canyon air temperature.

222

223

224

225

226

227

228

229

230

231

232

233

234

235

236

237

238

239

240

241

242

243

244

As shown in Fig. 3b, the change in bare soil fraction (f_S) has marginal cooling effect. In contrast, the cooling efficiency from irrigation is significant, especially for cities in hot and dry climate (Crawford et al., 2012; Wang et al., 2019). The impact of irrigation on carbon exchange, on the other hand, is highly nonlinear. Two distinct regions can be identified in Fig. 3b: the contour lines are steep at the low soil moisture regime ($SWC_x < 1.3$) but plateaued when amply irrigated, indicating the sharp change of sensitivity of carbon uptake to irrigation. As approaching the limiting case where irrigation is turned off, the high water stress suppresses the carbon uptake from plants, leaving bare soil respiration the primary source of CO_2 exchange. The

rate of soil respiration is positively correlated with a wide range of soil temperature (Lloyd and Taylor 1994). When urban plants are irrigated, it clearly provides the co-benefit of cooling the ambient air temperature (Fig. 3a), and meanwhile reducing the CO_2 emission by (1) reducing soil respiration via cooling effect and (2) promoting plant carbon absorption via reducing the water stress. When adequately irrigated ($SWC_x > 2.0$), the CO_2 uptake becomes insensitive to further increase in irrigation amount, and the net carbon flux is in turn dominated by the change of bare soil fraction (c.f. flat contour lines in Fig. 3b).

245

246

247

248

249

250

251

252

253

254

255

256

257

258

259

260

261

262

263

264

265

266

267

For results shown in Fig. 3a and 3b, we keep the land cover changing independently, meaning that the increase of f_S and f_V leads to the decrease of total impervious surface area (ISA). In practical urban planning, however, the ISA is unlikely to change, at least significantly, in a developed built environment. To capture the more realistic urban greening strategies, we then devise an alternative set of scenarios by fixing the total fraction of urban greening at 30% (i.e. fs $+ f_V = 0.3$). The changes of lawn and bare soil fractions are therefore dependent and limited to the availability of open ground space in the street canyon. Urban greening at the road level physically represents the conversion of bare soil into vegetated surface, or reversely as the degradation of urban lawns. The simulation results of the effect of this new (and more realistic) set of urban greening scenarios on urban cooling and carbon mitigation are shown in Fig. 3c&d, and can be seen as qualitatively consistent with the results of their counterpart scenarios in Fig. 3a&b. Nevertheless, some differences are noted: first, the increase of fy in Fig. 3c leads to faster carbon mitigation rate by increasing vegetation cover than that in Fig. 3a. This is due to that urban greening, by converting bare soil to vegetated (with a constant availability of open space in the street canyon), is doubly beneficial by providing additional CO₂ uptake capability as well as evaporative cooling (Song and Wang 2015; Aram et al., 2019), both contributing to CO₂

reduction. Similar trend of strengthened carbon mitigation capacity can be found, by comparing Fig. 3d and 3b, via enhanced irrigation of urban lawns.

It is noteworthy that from reported observation dataset, soil respiration from vegetated area is higher than that arising from purely bare soils, primarily because of active root respiration and high soil organic carbon from the grassland (Ng et al., 2015; Tao et al., 2016; Bae and Ryu 2017). Nevertheless, well-maintained urban lawns act net CO₂ sinks, despite that the elevated soil respiration rate weakens the plant carbon uptake. This effect will be further amplified if an urban lawn degrades into brown turf grassland with large bare soil portion due to extreme heat or drought, as the vegetation fraction for active CO₂ uptake shrinks while respiration from underground biomass continues.

Furthermore, the results of predicted sensible and latent heat fluxes aggregated over the street canyon are shown in Fig. 4. The response of sensible heat to varying components of urban greening is similar to that of the canyon air temperature, and the latent heat to carbon likewise. It is noteworthy that in Fig. 4b, the latent heat exhibits a bi-modal pattern with respect to the bare soil fraction in the regime where the soil moisture is high ($SWC_x > 2.2$). This bimodal pattern of latent heat can be attributed to two mechanisms regulating plant transpiration and soil evaporation separately. When the bare soil fraction is low ($f_S < 0.05$), the presence of large impervious surface warms the canyon air (Fig. 3b), which can, in turn, enhances plant evapotranspiration with ample irrigation. On the other extremity, when the large bare soil fraction is large ($f_S > 0.15$), urban irrigation leads to large soil evaporation.

3.2.2 Diurnal variation of changes in temperature and carbon flux

In addition to the mean heat and carbon mitigation, here we look into the diurnal variation of $T_{\rm can}$ and NEE_{can} due to urban greening by presenting the results of a portfolio of selected scenarios listed in Table 2, as shown in Fig. 5. From Fig. 5a, it can be seen that the increase of ground vegetation fraction can enhance the strength of CO₂ sink, but has insignificant impact on environmental cooling. Furthermore, the use of lawns for mitigating carbon emissions is subject to additional constraints: (1) irrigation of urban lawns, or more generally the maintenance of mesic landscaping, in the semi-arid or arid cities can be demanding due to water scarcity (Litvak et al., 2017), and (2) lawns are susceptible to degradation from exposure to high thermal and water stresses. In contrast, urban trees provide an attractive means as they provide more significant cooling effect (Fig. 5b), especially during nighttime (recall that UHI is predominantly a nocturnal effect), owing to the synergistic radiative and evapotranspirative cooling (Konarska et al., 2016; Upreti et al., 2017; Wang et al., 2018; Wang et al., 2019). Increasing tree fraction also promotes CO₂ sequestration significantly during daytime. The significant carbon sink strength of trees is primarily attributable to greater leaf areas in multiple layers of tree canopy and wide adaptation to heat and water stress (Teskey et al., 2015). For cities in arid environment, shade trees (especially native species) are particularly recommendable for better environmental co-benefit of thermal and carbon mitigation and more economic water-heat trade-off.

290

291

292

293

294

295

296

297

298

299

300

301

302

303

304

305

306

307

308

309

310

311

312

As comparing to the reference case, increased irrigation does not intend to significantly reduce $T_{\rm can}$ or NEE_{can}. But less irrigation will lead to apparent temperature increase and loss of CO₂ sequestration (Fig. 5d). The normalized saturation degree ($S_{\rm norm}$) for Irr⁻, Ref, and Irr⁺ cases are about 5%, 30% and 70%, respectively. The asymmetric phenomenon is likely caused by the non-linear relationship of evapotranspiration as a function of soil moisture (ET- θ relation) (Li and Wang 2019). When soil moisture becoming the limiting factor for plant growth, evaporative

cooling and CO_2 uptake will be largely suppressed. On the contrary, when soil moisture is adequate to support healthy growth for plants, T_{can} becomes insensitive to irrigation, so does NEE_{can} . The diurnal variation echoes the mean effect discussed in the previous section: Adequate irrigation is necessary to effectuate the environmental co-benefit of urban greening for heat and carbon mitigation, whereas excessive soil water only has but marginal effect on further improving the urban environmental quality.

3.3 Implications to environmental management

Based on results derived from the designed scenarios, urban greening, in general, leads to the improvement of thermal and carbon environment in cities. Though theoretically, wide coverage of green space and irrigation cool the environment and strengthen natural carbon sinks to a significant degree, cost-benefit trade-offs should be considered in management practices. It is noteworthy that the benefit evaluation should take the value of carbon sinks into account. From this perspective, the cost of irrigation will be offset by the added value it creates in CO₂ emission reduction, as it 1) helps vegetation maintain a healthy status for active CO₂ uptake; 2) mitigates the degradation risk of urban lawns; 3) cools the soil thus suppress soil respiration. Similarly, it is recommended to adopt street trees, instead of lawns, for better heat and CO₂ emission mitigation effects in cities, as tree 1) has denser leaves thus greater CO₂ sink power; 2) cools the environment thus suppress respiration; 3) requires less maintenance. Nonetheless, for some specific regions or tree species, trees might be exposed to other risks such as wildfire (Dass et al., 2018) and mortality (Smith et al., 2019; Hilbert et al., 2019).

Quantitatively, the interplays between thermal and carbon environment need to be disentangled using advanced numerical models. For example, both temperature and moisture

control the microbial activity in the soil, thus irrigation amount determines whether co-benefits or advisory effects happen in practice. Despite the fact that irrigation cools the soil, extra soil moisture might promote soil respiration. Meanwhile, insufficient irrigation affects the growth of vegetation and limits the photosynthesis rate. Best environmental co-benefits will be achieved when the fine balance between these mechanisms is found. The critical thresholds will vary from different cities, local tree species, and management practices. For cities in arid climate regions where urban thermal stress and water scarcity co-exist, results from precise modeling might refresh the perspectives on cost-benefit trade-offs, therefore unveil more feasible strategies to a low carbon city. Urban planners and city designers should also adopt the modeling tools from urban climate research communities in decision-making progresses.

4 Concluding remarks

Urban greening strategies are widely used by urban planners, practitioners, and researchers as an effective and aesthetically appealing means to promote the thermal and air quality in urban areas, and sustainable development of cities in the future. The functioning and efficacy of urban greening strategies involve complex interactions between landscape dynamics, anthropogenic activities, and atmospheric transport, which leads to compound, rather than singular, environmental impacts embracing the co-benefits and potential trade-offs among heat, carbon, and pollution mitigation.

To quantify the compound environmental co-benefits induced by urban greenery, in this study, we applied a newly developed UCM-CO₂ model to quantify the relative contribution of heat and carbon mitigation arising from specific components of urban greening, viz. grassland, tree, soil, and irrigation. It was found that tall shades trees are the most effective for cooling and

reducing the net carbon emissions but can also potentially suppress the carbon uptake by vegetation at the ground level. In contrast, the effect of mesic landscape using urban lawns is conditioned on the adequate water supply and good maintenance practices to prevent degradation, whereas xeriscaping has limited capacity for reducing carbon emissions despite its water-saving potential. In addition, we identified the nonlinear transition in the response of ambient temperature (while the room temperature is kept at constant 25°C) and total carbon flux, and the bi-modal variability of the latent heat, to different irrigation schemes.

Moreover, the algorithms of the UCM-CO₂ model and the proposed method in this study are generic and easily portable to be applied to other cities in diverse geographic and climatic regions. For example, the model capacity and the finding of these intriguing patterns of irrigation enable urban planners and practitioners to optimize urban irrigation strategies in terms of the water-energy trade-off. More generally, the proposed method can be extended to study compound environmental impacts of generic urban sustainable solutions, in terms of their cobenefit, trade-offs, and unintended consequence by modifying ambient temperatures, building energy consumption, air quality, greenhouse gas emission, human health, and biodiversity. Finding of these compound effects will, in turn, improve our understanding of the holistic urban livability and foster the practices of sustainable urban environmental management.

Acknowledgement

This study is based upon work supported by the US National Science Foundation (NSF) under grants AGS-1930629 and CBET-2028868, and the National Aeronautics and Space Administration (NASA) under grant 80NSSC20K1263. We acknowledge the Central Arizona-Phoenix Long-Term Ecological Research (CAP LTER) project under NSF grant # DEB-1637590

- for providing the field measurement. Data used in this study is available at
- $\underline{\text{https://sustainability.asu.edu/caplter/research/long-term-monitoring/urban-flux-tower/.}$

Table 1. Summary of the parameter space used in UCM-CO₂ for the study site in Phoenix, Arizona.

Site Properties		
Roof level (m)	4.5	
Reference height (m)	22.1	
Normalized roof height (-)	0.1	
Normalized roof width (-)	0.4	
Normalized road width (-)	0.6	
Thickness of roof (m)	0.3	
Thickness of wall (m)	0.2	
Roughness length for momentum for roof (m)	0.01	
Roughness length for momentum for canyon (m)	0.05	
Roughness length for heat for roof (m)	0.001	
Roughness length for heat for canyon (m)	0.005	
Street canyon orientation (rad)	3/8 π	
Latitude (rad)	0.5844	
Longitude (rad)	1.9573	
Soil Properties		
Saturation hydraulic conductivity (m s ⁻¹)	3.4 x 10 ⁻⁵	
Residual soil water content (m³m-³)	0.08	
Saturated soil water content (m ³ m ⁻³)	0.35	
Slope of soil water retention curve, b	4.50	
Soil layer thickness (m)	0.15	
Surface Properties		
Roof		
Albedo	0.13	
Emissivity	0.95	
Thermal conductivity (W K ⁻¹ m ⁻¹)	0.90	
Heat capacity (MJ K ⁻¹ m ⁻³)	1.00	
Wall		
Albedo	0.40	
Emissivity	0.95	
Thermal conductivity (W K ⁻¹ m ⁻¹)	0.10	
Heat capacity (MJ K ⁻¹ m ⁻³)	1.40	
Road (soil, paved, vegetation)		
Fractions	0.37, 0.53, 0.10	
Albedo	0.30, 0.25, 0.30	
Emissivity	0.95, 0.95, 0.95	
Thermal conductivity (W K ⁻¹ m ⁻¹)	1.50, 1.80, 1.00	
Heat capacity (MJ K ⁻¹ m ⁻³)	1.80, 1.80, 1.70	
Tree		
Coverage	0.05	
Normalized tree height (-)	0.80	
Normalized tree location (-)	0.10	
LAI $(m^2 m^{-2})$	4.5	

Table 2. Configurations of urban greening for the study site and numerical experimental scenarios

Scenario	f_V	f_T	f_S	SWC_{x}
PHX	0.10	0.05	0.37	1.5
Ref	0.15	0.15	0.15	2.0
Grass-	0.05	0.15	0.15	2.0
$Grass^+$	0.25	0.15	0.15	2.0
Tree-	0.15	0.05	0.15	2.0
Tree ⁺	0.15	0.25	0.15	2.0
Soil ⁻	0.15	0.15	0.05	2.0
$Soil^+$	0.15	0.15	0.25	2.0
Irr-	0.15	0.15	0.15	1.0
Irr ⁺	0.15	0.15	0.15	3.0

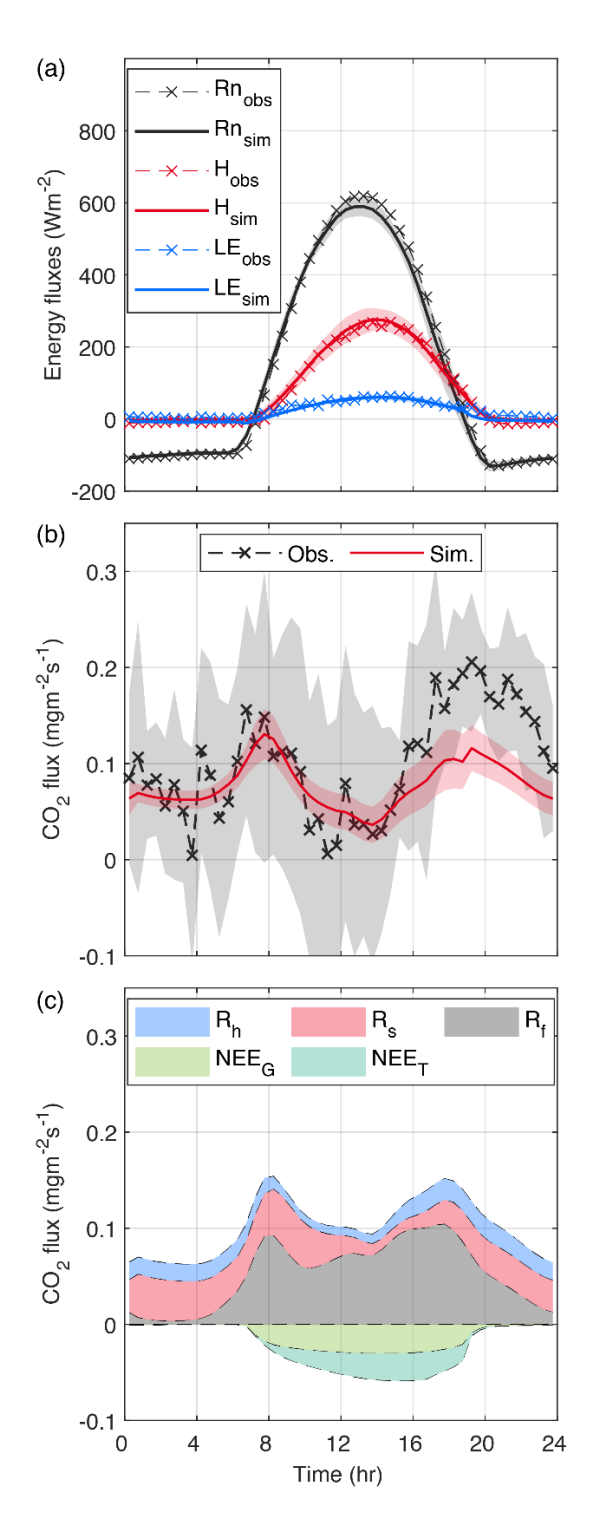


Figure 1. Comparison of model results with field measurements by the EC tower: (a) surface energy fluxes; (b) total CO_2 flux. Shades represent one standard deviation from the model and observation mean. (c) decomposition of total CO_2 flux from UCM- CO_2 model. R_h , R_s , and R_f

represent respiration from human activity, soil, fossil fuel combustion, respectively. NEE_G and NEE_T represent NEE from urban lawn and tree, respectively.



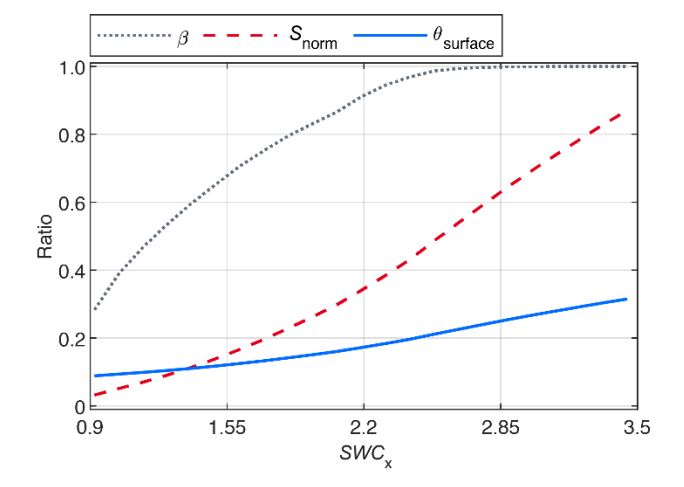


Figure 2. Relation between SWC_x to evaporation reduction factor (β , black dot line), normalized saturation degree (S_{norm} , red dash line), and surface soil moisture ($\theta_{surface}$, blue solid line). β is defined as the actual ET rate to the potential ET. S_{norm} = (surface soil moisture – wilting point) / (field capacity – wilting point). In this case, the field capacity and wilting point are 0.35 and 0.08, respectively.

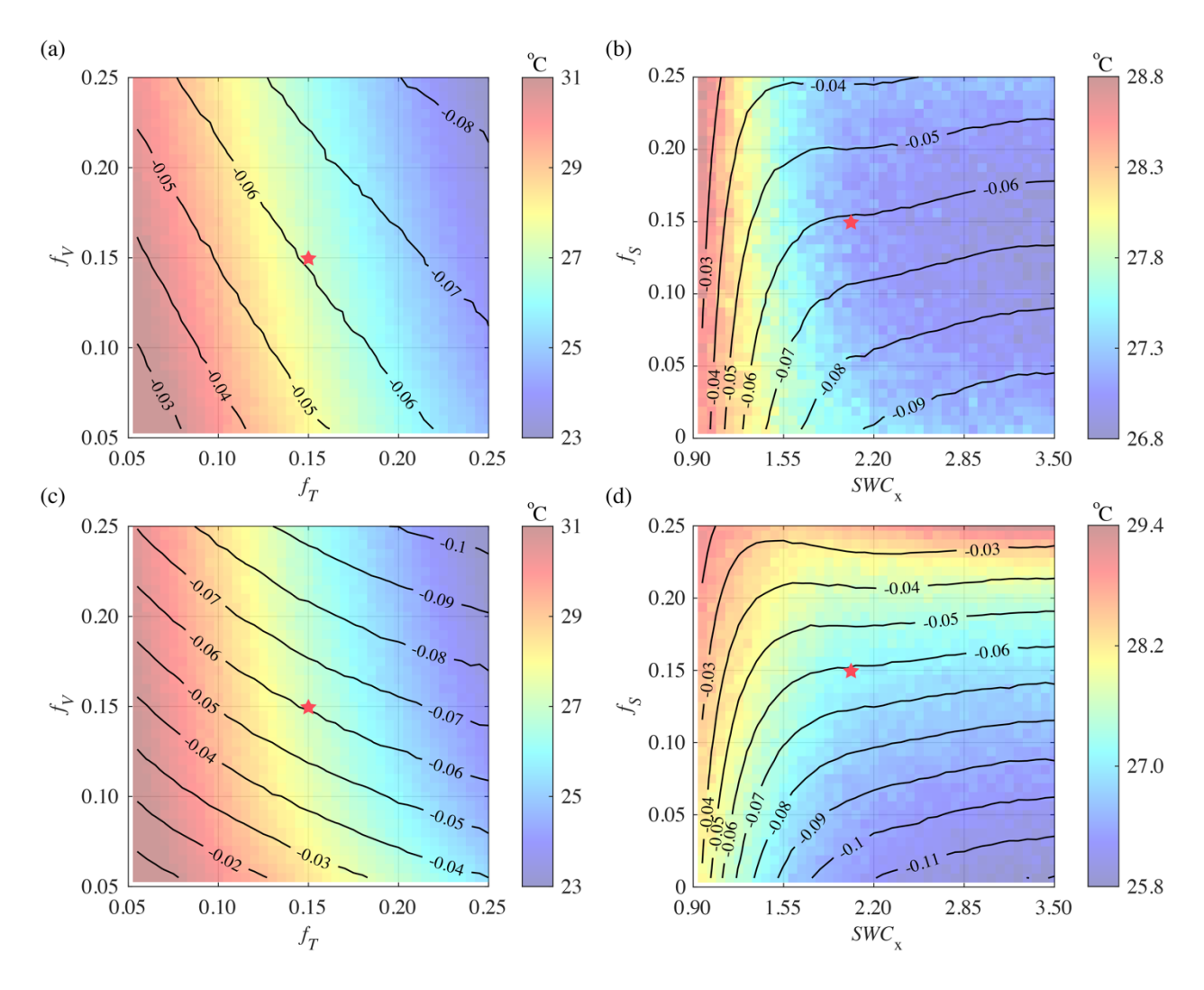


Figure 3. Simulation results of the mean canyon air temperature (T_{can} in ${}^{\circ}$ C, filled colormap) and net biogenic CO₂ exchange (NEE_{can} in mg m⁻²s⁻¹, contours) by changing (a) tree coverage, f_T and grassland fraction, f_V , and (b) bare soil fraction, f_S and irrigation schedule, SWC_x , independently. Subplots (c) and (d) are the same as (a) and (b) but keeping the total fraction of $f_V + f_S$ as constant of 0.3. The star indicates the reference scenario with $f_V = 0.15$, $f_T = 0.15$, $f_S = 0.15$, $SWC_x = 2.0$.

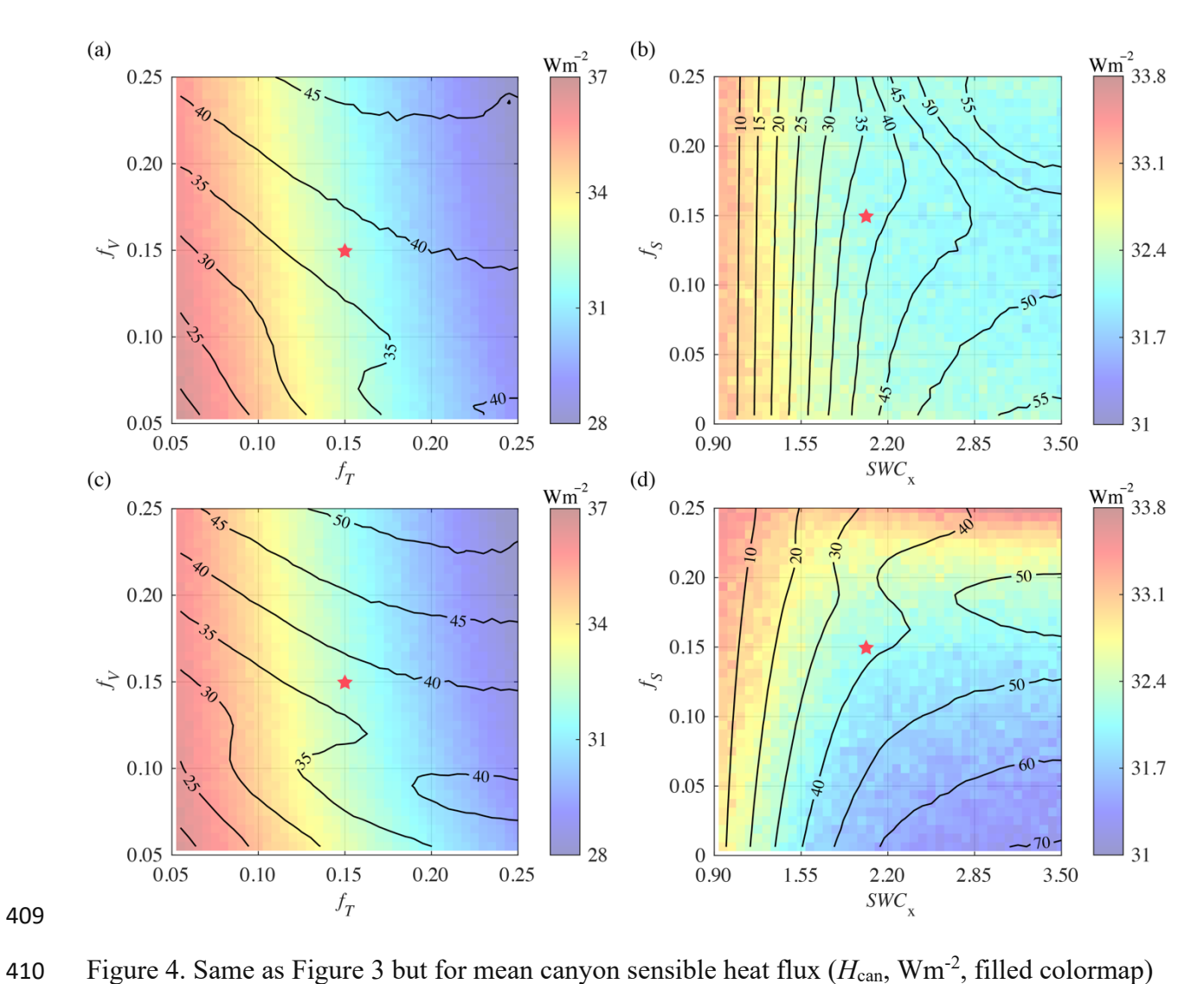


Figure 4. Same as Figure 3 but for mean canyon sensible heat flux (H_{can} , Wm⁻², filled colormap) and latent heat flux (LEcan, Wm⁻², contours).

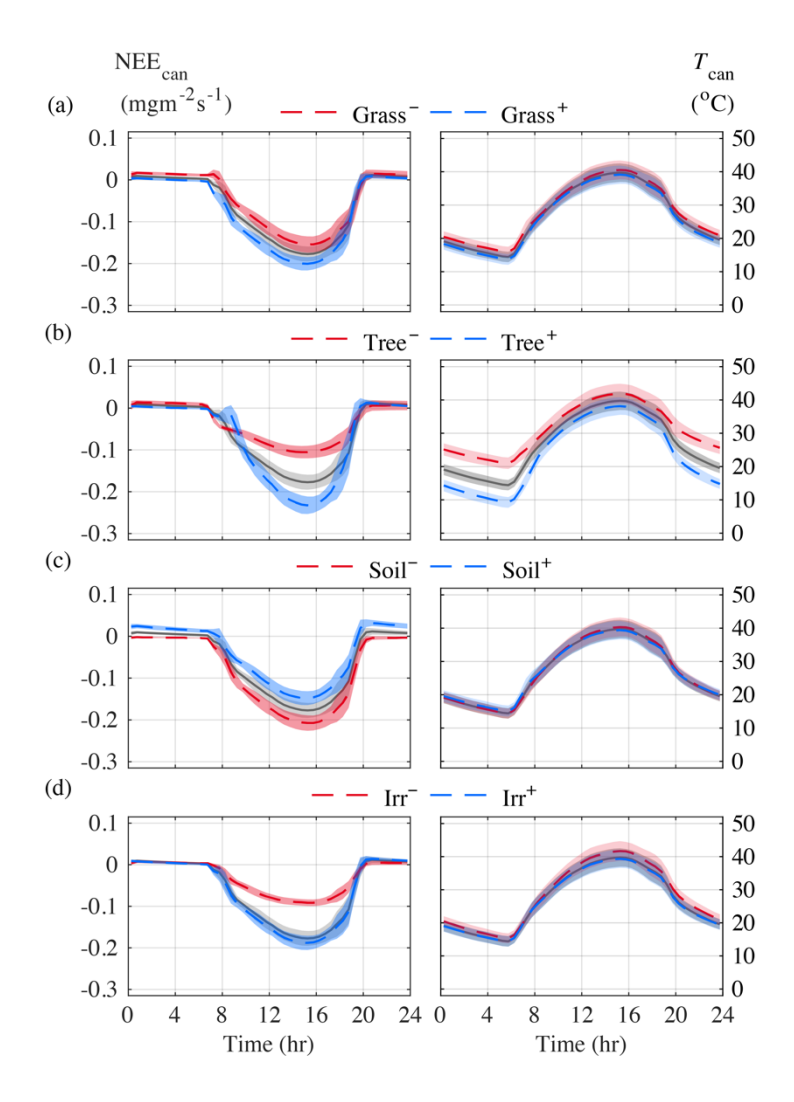


Figure 5. Mean diurnal variation of the net biogenic CO₂ exchange NEE_{can} and the canyon temperature T_{can} : (a) Grass[±], (b) Tree[±], (c) Soil[±], and (d) Irr[±]. Blue and red lines stand for the "+" and "–" scenarios in each category, respectively (detailed in Table 2). Shaded areas represent one standard deviation. The solid black line indicates the reference scenario with $f_V = 0.15$, $f_T = 0.15$, $f_S = 0.15$, $SWC_x = 2.0$.

Reference

- Aram, F., Higueras García, E., Solgi, E. and Mansournia, S., 2019. Urban green space cooling
- effect in cities. *Heliyon* **5** 4 e01339-e01339. http://doi.org/10.1016/j.heliyon.2019.e01339
- 421 Arnfield, A.J., 2003. Two decades of urban climate research: a review of turbulence, exchanges
- of energy and water, and the urban heat island. *Int. J. Clim.* **23** 1 1-26.
- 423 http://doi.org/10.1002/joc.859
- Bae, J. and Ryu, Y., 2017. Spatial and temporal variations in soil respiration among different
- land cover types under wet and dry years in an urban park. Landsc. Urban Plan. 167 378-
- 426 385. http://doi.org/10.1016/j.landurbplan.2017.07.020
- Bergeron, O. and Strachan, I.B., 2011. CO2 sources and sinks in urban and suburban areas of a
- 428 northern mid-latitude city. *Atmos. Environ.* **45** 8 1564-1573.
- 429 http://doi.org/10.1016/j.atmosenv.2010.12.043
- Bowler, D.E., Buyung-Ali, L., Knight, T.M. and Pullin, A.S., 2010. Urban greening to cool
- towns and cities: A systematic review of the empirical evidence. Landsc. Urban Plan. 97 3
- 432 147-155. http://doi.org/10.1016/j.landurbplan.2010.05.006
- Chow, W.T.L. and Brazel, A.J., 2012. Assessing xeriscaping as a sustainable heat island
- mitigation approach for a desert city. *Build Environ.* **47** 170-181.
- 435 http://doi.org/10.1016/j.buildenv.2011.07.027
- 436 Chow, W.T.L., Volo, T.J., Vivoni, E.R., Jenerette, G.D. and Ruddell, B.L., 2014. Seasonal
- dynamics of a suburban energy balance in Phoenix, Arizona. *Int. J. Clim.* **34** 15 3863-3880.
- 438 http://doi.org/10.1002/joc.3947
- Christen, A., Coops, N.C., Crawford, B.R., Kellett, R., Liss, K.N., Olchovski, I., ... Voogt, J.A.,
- 2011. Validation of modeled carbon-dioxide emissions from an urban neighborhood with

direct eddy-covariance measurements. Atmos. Environ. 45 33 6057-6069. 441 http://doi.org/https://doi.org/10.1016/j.atmosenv.2011.07.040 442 Churkina, G., 2016. The Role of Urbanization in the Global Carbon Cycle. Front. Ecol. Evol. 3, 443 144. http://doi.org/10.3389/fevo.2015.00144 444 Contosta, A.R., Lerman, S.B., Xiao, J. and Varner, R.K., 2020. Biogeochemical and 445 446 socioeconomic drivers of above- and below-ground carbon stocks in urban residential yards of a small city. Landsc. Urban Plan. 196 103724. 447 http://doi.org/10.1016/j.landurbplan.2019.103724 448 449 Crawford, A.J., McLachlan, D.H., Hetherington, A.M. and Franklin, K.A., 2012. High temperature exposure increases plant cooling capacity. Curr. Biol. 22 10 R396-397. 450 http://doi.org/10.1016/j.cub.2012.03.044 451 Crawford, B., Grimmond, C.S.B. and Christen, A., 2011. Five years of carbon dioxide fluxes 452 measurements in a highly vegetated suburban area. Atmos. Environ. 45 4 896-905. 453 454 http://doi.org/10.1016/j.atmosenv.2010.11.017 Dass, P., Houlton, B., Wang, Y. and Warlind D., 2018. Grasslands may be more reliable carbon 455 sinks than forests in California. Environ. Res. Lett. 13 074027. http://doi.org/10.1088/1748-456 457 9326/aacb39 Decina, S.M., Hutyra, L.R., Gately, C.K., Getson, J.M., Reinmann, A.B., Short Gianotti, A.G. 458 and Templer, P.H., 2016. Soil respiration contributes substantially to urban carbon fluxes in 459 460 the greater Boston area. Environ. Pollut. 212 433-439. http://doi.org/10.1016/j.envpol.2016.01.012 461

Dyukarev, E.A., 2017. Partitioning of net ecosystem exchange using chamber measurements data 462 from bare soil and vegetated sites. Agric. For. Meteorol. 239 236-248. 463 http://doi.org/10.1016/j.agrformet.2017.03.011 464 Gately, C.K. and Hutyra, L.R., 2017. Large Uncertainties in Urban-Scale Carbon Emissions. J. 465 Geophys. Res. Atmos. 122 20 11242-11260. http://doi.org/10.1002/2017jd027359 466 467 Gately, C.K., Hutyra, L.R. and Sue Wing, I., 2015. Cities, traffic, and CO2: A multidecadal assessment of trends, drivers, and scaling relationships. Proc. Natl. Acad. Sci. U. S. A. 112 468 16 4999-5004. http://doi.org/10.1073/pnas.1421723112 469 470 Goret, M., Masson, V., Schoetter, R. and Moine, M.-P., 2019. Inclusion of CO2 flux modelling in an urban canopy layer model and an evaluation over an old European city centre. Atmos. 471 Environ. X3 http://doi.org/10.1016/j.aeaoa.2019.100042 472 Grimmond, C.S.B., Blackett, M., Best, M.J., Baik, J.J., Belcher, S.E., Beringer, J., ... Zhang, N., 473 2011. Initial results from Phase 2 of the international urban energy balance model 474 475 comparison. Int. J. Clim. **31** 2 244-272. http://doi.org/10.1002/joc.2227 Gurney, K.R., Mendoza, D.L., Zhou, Y., Fischer, M.L., Miller, C.C., Geethakumar, S. and de la 476 Rue du Can, S., 2009. High resolution fossil fuel combustion CO2 emission fluxes for the 477 478 United States. Environ. Sci. Technol. 43 14 5535-5541. http://doi.org/10.1021/es900806c Hilbert, D.R., Roman, L.A., Koeser, A.K., Vogt, J. and van Doorn, N.S., 2019. Urban tree 479 mortality: A literature review. Arboric. Urban For. 45 5 167-200. 480 481 http://doi.org/10.13140/RG.2.2.25953.15204 Hutyra, L.R., Duren, R., Gurney, K.R., Grimm, N., Kort, E.A., Larson, E. and Shrestha, G., 482

2014. Urbanization and the carbon cycle: Current capabilities and research outlook from

- the natural sciences perspective. *Earth's Future* **2** 10 473-495.
- 485 http://doi.org/10.1002/2014ef000255
- Järvi, L., Havu, M., Ward, H.C., Bellucco, V., McFadden, J.P., Toivonen, T., ... Grimmond,
- 487 C.S.B., 2019. Spatial Modeling of Local-Scale Biogenic and Anthropogenic Carbon
- Dioxide Emissions in Helsinki. J. Geophys. Res. Atmos. 124 15 8363-8384.
- 489 http://doi.org/10.1029/2018jd029576
- Koerner, B. and Klopatek, J., 2002. Anthropogenic and natural CO2 emission sources in an arid
- 491 urban environment. *Environ. Pollut.* **116** S45-S51.
- 492 http://doi.org/https://doi.org/10.1016/S0269-7491(01)00246-9
- Konarska, J., Uddling, J., Holmer, B., Lutz, M., Lindberg, F., Pleijel, H. and Thorsson, S., 2016.
- Transpiration of urban trees and its cooling effect in a high latitude city. *Int. J.*
- 495 *Biometeorol.* **60** 1 159-172. http://doi.org/10.1007/s00484-015-1014-x
- Landscape Watering by Numbers, 2017. Retrieved from https://wateruseitwisely.com/100-ways-
- 497 to-conserve/landscape-watering-guide/
- Li, P. and Wang, Z.-H., 2019. Estimating evapotranspiration over vegetated surfaces based on
- wet patch patterns. *Hydrol. Res.* **50** 4 1037-1046. http://doi.org/10.2166/nh.2019.034
- Li, P. and Wang, Z.-H., 2020. Modeling carbon dioxide exchange in a single-layer urban canopy
- model. *Build Environ*. **184** http://doi.org/10.1016/j.buildenv.2020.107243
- Li, P. and Wang, Z.-H., 2021. Uncertainty and sensitivity analysis of modeling plant CO2
- exchange in the built environment. *Build Environ.* **189** 107539.
- 504 http://doi.org/https://doi.org/10.1016/j.buildenv.2020.107539

- Litvak, E., Manago, K.F., Hogue, T.S. and Pataki, D.E., 2017. Evapotranspiration of urban
- landscapes in Los Angeles, California at the municipal scale. *Water Resour. Res.* **53** 5
- 507 4236-4252. http://doi.org/10.1002/2016wr020254
- Lloyd, J. and Taylor, J.A., 1994. On the Temperature Dependence of Soil Respiration. *Funct*.
- 509 *Ecol.* **8** 3 315-323. http://doi.org/10.2307/2389824
- Meili, N., Manoli, G., Burlando, P., Bou-Zeid, E., Chow, W.T.L., Coutts, A.M., . . . Fatichi, S.,
- 511 2020. An urban ecohydrological model to quantify the effect of vegetation on urban
- climate and hydrology (UT&C v1.0). *Geosci. Model Dev.* **13** 1 335-362.
- 513 http://doi.org/10.5194/gmd-13-335-2020
- Ng, B.J.L., Hutyra, L.R., Nguyen, H., Cobb, A.R., Kai, F.M., Harvey, C. and Gandois, L., 2015.
- Carbon fluxes from an urban tropical grassland. *Environ. Pollut.* **203** 227-234.
- 516 http://doi.org/10.1016/j.envpol.2014.06.009
- O'Malley, C., Piroozfar, P., Farr, E.R.P. and Pomponi, F., 2015. Urban Heat Island (UHI)
- mitigating strategies: A case-based comparative analysis. *Sustain. Cities Soc.* **19** 222-235.
- 519 http://doi.org/10.1016/j.scs.2015.05.009
- Oda, T., Maksyutov, S. and Andres, R.J., 2018. The Open-source Data Inventory for
- Anthropogenic CO2, version 2016 (ODIAC2016): a global monthly fossil fuel CO2
- gridded emissions data product for tracer transport simulations and surface flux inversions.
- 523 Earth Syst. Sci. Data 10 1 87-107. http://doi.org/10.5194/essd-10-87-2018
- Oke, T.R., 1973. City size and the urban heat island. *Atmos. Environ.* 7 8 769-779.
- 525 http://doi.org/https://doi.org/10.1016/0004-6981(73)90140-6
- Oke, T.R., 1982. The energetic basis of the urban heat island. Q. J. R. Meteorol. Soc. 108 455 1-
- 527 24. http://doi.org/https://doi.org/10.1002/qj.49710845502

- Oke, T.R., Mills, G., Christen, A. and Voogt, J.A. (2017). <u>Urban Climates</u>. Cambridge,
- 529 Cambridge University Press.
- Perkins, S.E., 2015. A review on the scientific understanding of heatwaves—Their measurement,
- driving mechanisms, and changes at the global scale. *Atmos. Res.* **164** 242-267.
- 532 http://doi.org/10.1016/j.atmosres.2015.05.014
- Ryu, Y.-H., Bou-Zeid, E., Wang, Z.-H. and Smith, J.A., 2016. Realistic Representation of Trees
- in an Urban Canopy Model. *Boundary Layer Meteorol.* **159** 2 193-220.
- 535 http://doi.org/10.1007/s10546-015-0120-y
- Sailor, D.J., 2011. A review of methods for estimating anthropogenic heat and moisture
- emissions in the urban environment. *Int. J. Clim.* **31** 2 189-199.
- 538 http://doi.org/https://doi.org/10.1002/joc.2106
- Sailor, D.J. and Lu, L., 2004. A top-down methodology for developing diurnal and seasonal
- anthropogenic heating profiles for urban areas. *Atmos. Environ.* **38** 17 2737-2748.
- 541 http://doi.org/https://doi.org/10.1016/j.atmosenv.2004.01.034
- Sargent, M., Barrera, Y., Nehrkorn, T., Hutyra, L.R., Gately, C.K., Jones, T., ... Wofsy, S.C.,
- 543 2018. Anthropogenic and biogenic CO₂ fluxes in the Boston urban region. *Proc. Natl.*
- 544 Acad. Sci. U. S. A. 115 29 7491-7496. http://doi.org/10.1073/pnas.1803715115
- 545 Smith, I.A., Dearborn, V.K. and Hutyra, L.R., 2019. Live fast, die young: Accelerated growth,
- mortality, and turnover in street trees. *PLOS ONE* **14** 5 e0215846.
- 547 http://doi.org/10.1371/journal.pone.0215846
- Song, J. and Wang, Z.-H., 2015. Impacts of mesic and xeric urban vegetation on outdoor thermal
- comfort and microclimate in Phoenix, AZ. *Build Environ.* **94** 558-568.
- 550 http://doi.org/10.1016/j.buildenv.2015.10.016

Song, J. and Wang, Z.-H., 2016. Diurnal changes in urban boundary layer environment induced 551 by urban greening. Environ. Res. Lett. 11 114018 http://doi.org/10.1088/1748-552 9326/11/11/114018 553 Still, C.J., Berry, J.A., Collatz, G.J. and DeFries, R.S., 2003. Global distribution of C3 and 554 C4vegetation: Carbon cycle implications. Global Biogeochem. Cycles 17 1 6-1-6-14. 555 556 http://doi.org/10.1029/2001gb001807 Tao, X., Cui, J., Dai, Y., Wang, Z. and Xu, X., 2016. Soil respiration responses to soil 557 physiochemical properties in urban different green-lands: A case study in Hefei, China. Int. 558 559 Soil Water Conserv. Res. 4 3 224-229. http://doi.org/10.1016/j.iswcr.2016.08.001 Teskey, R., Wertin, T., Bauweraerts, I., Ameye, M., McGuire, M.A. and Steppe, K., 2015. 560 Responses of tree species to heat waves and extreme heat events. Plant Cell Environ. 38 9 561 1699-1712. http://doi.org/10.1111/pce.12417 562 Trammell, T.L.E., Pataki, D.E., Still, C.J., Ehleringer, J.R., Avolio, M.L., Bettez, N., . . . 563 Wheeler, M.M., 2019. Climate and lawn management interact to control C4 plant 564 distribution in residential lawns across seven U.S. cities. Ecol. Appl. 29 4 e01884. 565 http://doi.org/10.1002/eap.1884 566 567 United Nations, 2019. World urbanization prospects - the 2018 revision. New York, Department of Economic and Social Affairs. 568 569 Upreti, R., Wang, Z.-H. and Yang, J., 2017. Radiative shading effect of urban trees on cooling 570 the regional built environment. Urban Forestry and Urban Greening 26 18-24. http://doi.org/10.1016/j.ufug.2017.05.008 571

- Velasco, E. and Roth, M., 2010. Cities as Net Sources of CO2: Review of Atmospheric CO2
- Exchange in Urban Environments Measured by Eddy Covariance Technique. *Geogr.*
- 574 *Compass* 4 9 1238-1259. http://doi.org/10.1111/j.1749-8198.2010.00384.x
- Velasco, E., Roth, M., Tan, S.H., Quak, M., Nabarro, S.D.A. and Norford, L., 2013. The role of
- vegetation in the CO2 flux from a tropical urban neighbourhood. *Atmos. Chem. Phys.* **13** 20
- 577 10185-10202. http://doi.org/10.5194/acp-13-10185-2013
- Vesala, T., Kljun, N., Rannik, U., Rinne, J., Sogachev, A., Markkanen, T., . . . Leclerc, M.Y.,
- 579 2008. Flux and concentration footprint modelling: state of the art. *Environ. Pollut.* **152** 3
- 580 653-666. http://doi.org/10.1016/j.envpol.2007.06.070
- Wang, C., Wang, Z.-H. and Ryu, Y.-H., 2021. A single-layer urban canopy model with
- transmissive radiation exchange between trees and street canyons. *Build Environ.* 191
- 583 107593. http://doi.org/https://doi.org/10.1016/j.buildenv.2021.107593
- Wang, C., Wang, Z.-H. and Sun, L., 2020. Early-Warning Signals for Critical Temperature
- Transitions. *Geophys. Res. Lett.* **47** 14 e2020GL088503.
- 586 http://doi.org/https://doi.org/10.1029/2020GL088503
- Wang, C., Wang, Z.-H., Wang, C. and Myint, S.W., 2019. Environmental cooling provided by
- urban trees under extreme heat and cold waves in U.S. cities. *Remote Sens. Environ.* 227
- 589 28-43. http://doi.org/10.1016/j.rse.2019.03.024
- Wang, C., Wang, Z.-H. and Yang, J., 2018. Cooling effect of urban trees on the built
- environment of contiguous United States. *Earth's Future* **6** 8 1066-1081.
- 592 http://doi.org/10.1029/2018EF000891
- Wang, Z.-H., 2014. Monte Carlo simulations of radiative heat exchange in a street canyon with
- 594 trees. Solar Energy 110 704-713. http://doi.org/10.1016/j.solener.2014.10.012

Wang, Z.-H., Bou-Zeid, E. and Smith, J.A., 2013. A coupled energy transport and hydrological 595 model for urban canopies evaluated using a wireless sensor network. Q. J. R. Meteorol. 596 Soc. 139 675 1643-1657. http://doi.org/https://doi.org/10.1002/qj.2032 597 Wang, Z.-H. and Upreti, R., 2019. A scenario analysis of thermal environmental changes 598 induced by urban growth in Colorado River Basin, USA. Landsc. Urban Plan. 181 125-599 600 138. http://doi.org/https://doi.org/10.1016/j.landurbplan.2018.10.002 Wang, Z.-H., Zhao, X., Yang, J. and Song, J., 2016. Cooling and energy saving potentials of 601 shade trees and urban lawns in a desert city. Appl. Energy 161 437-444. 602 http://doi.org/10.1016/j.apenergy.2015.10.047 603 Yang, J., Wang, Z.H., 2015a. Optimizing urban irrigation schemes for the trade-off between 604 energy and water consumption. Energy Build. 107 335-344. 605 https://doi.org/10.1016/j.enbuild.2015.08.045 606 Yang, J., Wang, Z.-H. and Kaloush, K.E., 2015b. Environmental impacts of reflective materials: 607 Is high albedo a 'silver bullet' for mitigating urban heat island? Renew. Sust. Energ. Rev. 608 47 830-843. http://doi.org/10.1016/j.rser.2015.03.092 609 Yang, J., Wang, Z.H., Georgescu, M., Chen, F., Tewari, M., 2016a. Assessing the impact of 610 611 enhanced hydrological processes on urban hydrometeorology with application to two cities in contrasting climates. J. Hydrometeorol. 17 1031-1047. https://doi.org/10.1175/JHM-D-612 613 15-0112.1 614 Yang, J., Wang, Z.H., Kaloush, K., Dylla, H., 2016b. Effect of pavement thermal properties on mitigating urban heat islands: A multi-scale modeling case study in Phoenix. Build. Env. 615 616 **108** 110-121. https://doi.org/10.1016/j.buildenv.2016.08.021

617	Ziter, C.D., Pedersen, E.J., Kucharik, C.J. and Turner, M.G., 2019. Scale-dependent interactions
618	between tree canopy cover and impervious surfaces reduce daytime urban heat during
619	summer. Proc. Natl. Acad. Sci. U. S. A. 116 15 7575-7580.
620	http://doi.org/10.1073/pnas.1817561116